An updated study of Υ production and polarization at the Tevatron and LHC *

FENG Yu(冯宇)[1)] GONG Bin(龚斌)[2)] WAN Lu-Ping(万露萍)[3)] WANG Jian-Xiong(王建雄)[4)]

Institute of High Energy Physics, Chinese Academy of Sciences, P.O.Box 918(4), Beijing 100049, China

Abstract: Following the nonrelativistic QCD factorization scheme, by taking the latest available measurements of $\chi_{bJ}(3P)$ into consideration, we present an updated study on the yield and polarization of $\Upsilon(1S, 2S, 3S)$ hadroproduction, and the fractions of $\chi_{bJ}(mP)$ feed-down in $\Upsilon(nS)$ production at QCD next-to-leading order. In the fitting, three schemes are applied with different choices of $\chi_{bJ}(mP)$ feed-down ratios and NRQCD factorization scale. The results can explain the measurements of yield very well. The polarization puzzle to $\Upsilon(3S)$ is now solved by considering the $\chi_{bJ}(3P)$ feed-down contributions. The ratio of $\sigma[\chi_{b2}(1P)]/\sigma[\chi_{b1}(1P)]$ measured by the CMS experiment can also be reproduced in our prediction. Among the different schemes, the results show little difference, but there are sizeable differences for the fitted long-distance color-octet matrix elements. This may bring large uncertainties when the values are applied in theoretical predictions for other experiments such as those at ee, ep colliders.

Key words: non-relativistic quantum chromodynamics, next-to-leading order, Υ, χ_{bJ} feed-down contributions, polarization

PACS: 12.38.Bx, 13.60.Le, 13.88.+e **DOI:** 10.1088/1674-1137/39/12/123102

1 Introduction

Quantum chromodynamics (QCD) successfully describes the strong interaction at parton level due to its property of asymptotic freedom, but it fails to calculate observations with detected hadrons directly since the hadronization from quarks is nonperturbative. Therefore, a factorization scheme to bridge the perturbative calculable part and nonperturbative hadronization part is crucial. For heavy quarkonium production and decay, the non-relativistic QCD (NRQCD) factorization scheme [1, 2], which was proposed to explain the huge discrepancy between the theoretical prediction and experimental measurements of the transverse momentum distribution of J/ψ production at the Tevatron, has been a very successful scheme in many applications. However, it encounters challenges in the transverse momentum distribution of polarization for J/ψ and Υ hadroproduction, where the theoretical predictions cannot describe the experimental measurements at QCD leading order (LO), or next-to-leading order (NLO).

In the last few years, significant progress has been made in NLO QCD calculations. The NLO corrections to color-singlet J/ψ hadroproduction were investigated in Refs. [3, 4], where the p_t distribution was found to be enhanced by two to three orders of magnitude in the high p_t region and the J/ψ polarization changes from transverse to longitudinal at NLO [4]. The results are reproduced at LO in a new factorization scheme for large p_t quarkonium production [5]. In Ref. [6], NLO corrections to J/ψ via S-wave color-octet (CO) states ($^1S_0^{[8]}$, $^3S_1^{[8]}$) were studied and the p_t distributions of both J/ψ yield and polarization found to change little compared with LO. The NLO corrections for χ_{cJ} hadroproduction were studied in Ref. [7]. Calculations and fits for both yield and polarization of J/ψ production at NLO QCD presented by three groups [8–10]. The complete prompt J/ψ hadroproduction study, which corresponds to the present available experimental measurements, was performed in Ref. [10] for the first time. The J/ψ polarization puzzle is still not fully understood. Recently, the LHCb Collaboration [11] published their measurement of η_c production.

Received 31 March 2015, Revised 8 July 2015

∗ Supported by National Nature Science Foundation of China (11475183) and Youth Innovation Promotion Association of CAS (2014010)

1) E-mail: yfeng@ihep.ac.cn

2) E-mail: twain@ihep.ac.cn

3) E-mail: wanlp@ihep.ac.cn

4) E-mail: jxwang@ihep.ac.cn

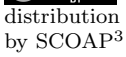

Three letters [12–14] came out successively, investigating the data from different points of view. Ref. [12] considered the η_c experiment as a challenge to NRQCD, while Refs. [13, 14] emphasized its indications on the J/ψ productions and polarizations. The complicated situation suggests that further study and phenomenological testing of NRQCD is still an urgent task.

ϒ production and polarization is one of the best alternative environments for understanding the physics in the hadronization of heavy quark pairs. Due to its heavier mass and smaller v (where v is the velocity of the heavy quark in the meson rest frame), one can expect better convergence in the QCD and NRQCD expansions, and consequently better description of the experiment by QCD NLO predictions. For ϒ hadroproduction, similar progress is also achieved in the p_t distribution of yield and polarization for the CS channel at QCD NLO [3, 4], and for S-wave CO states [15]. The NLO correction via all CO states is studied in Ref. [16]. The first complete NLO QCD corrections on yield and polarization of $\Upsilon(1S,\ 2S,\ 3S)$ are presented in our former work [17], where the results can explain the experimental measurements on yield very well, for the polarization of $\Upsilon(1S,2S)$ measured at the CMS experiment. However, without considering the $\chi_{bJ}(3P)$ feed-down contributions, the results for the polarization of $\Upsilon(3S)$ are inconsistent with data. Thereafter, the mass of $\chi_{bJ}(3P)$ was measured [18] at the LHC, and the fractions for $\Upsilon(3S)$ production from $\chi_{bJ}(3P)$ radiative decay were first measured [19] by the LHCb Collaboration. The large measured value of this fraction indicates that reconsideration of $\Upsilon(3S)$, as well as $\Upsilon(1S,\ 2S)$ is needed. In this work, we take into consideration the $\chi_{bJ}(3P)$ feed-down contributions carefully to update the yield and polarization analysis of $\Upsilon(nS)$ hadroproduction at QCD NLO correction, and also predict the ratio of differential cross sections of $\chi_{b2}(1P)$ to that of $\chi_{b1}(1P)$ from LHCb [18] and CMS [20].

This paper is organized as follows. In Section 2, we give a brief description of the theory in our work. Numerical results are presented in Section 3. In Section 4, we introduce more fitting schemes and discuss the difference between them. Finally, discussion and a summary are given in the last Section.

2 Theory description

Following the NRQCD factorization formalism [2], the cross section for quarkonium hadroproduction H can be expressed as

$$\mathrm{d}\sigma[\mathrm{pp}\to H+\mathrm{X}] = \sum_{\mathrm{i,j,n}}\int \mathrm{d}x_1\mathrm{d}x_2 G_{\mathrm{p}}^{\mathrm{i}} G_{\mathrm{p}}^{\mathrm{j}} \times \mathrm{d}\hat{\sigma}[\mathrm{ij}\to(\mathrm{b\overline{b}})_{\mathrm{n}}\mathrm{X}]\langle\mathcal{O}_{\mathrm{n}}^{\mathrm{H}}\rangle \quad (1)$$

where p is either a proton or an antiproton, $G_{\mathrm{p}}^{\mathrm{i(j)}}$ is the parton distribution function (PDF) of p, the indices i, j run over all possible partonic species, and n denotes the $\mathrm{b\overline{b}}$ intermediate states ($^3S_1^{[1]}$, $^1S_0^{[8]}$, $^3S_1^{[8]}$, $^3P_{\mathrm{J}}^{[8]}$) for ϒ and ($^3P_{\mathrm{J}}^{[1]}$, $^3S_1^{[8]}$) for χ_{bJ}. The short-distance coefficients $\mathrm{d}\hat{\sigma}$ can be calculated perturbatively, while the long-distance matrix elements(LDMEs) $\langle\mathcal{O}_{\mathrm{n}}^{\mathrm{H}}\rangle$ are governed by nonperturbative QCD effects.

The polarizations of ϒ are defined as [21]

$$\lambda=\frac{\mathrm{d}\sigma_{11}-\mathrm{d}\sigma_{00}}{\mathrm{d}\sigma_{11}+\mathrm{d}\sigma_{00}},\ \mu=\frac{\sqrt{2}\mathrm{Red}\sigma_{10}}{\mathrm{d}\sigma_{11}+\mathrm{d}\sigma_{00}},\ \nu=\frac{\sqrt{2}\mathrm{Red}\sigma_{1,-1}}{\mathrm{d}\sigma_{11}+\mathrm{d}\sigma_{00}}, \quad (2)$$

where $\mathrm{d}\sigma_{\mathrm{S_zS'_z}}$ is the spin density matrix of ϒ hadroproduction. Only the parameter λ in the helicity frame is considered in our work.

The fractions of $\Upsilon(nS)$ originating from $\chi_{\mathrm{bJ}}(mP)$ decays are defined as

$$\mathcal{R}^{\chi_{\mathrm{b}}(mp)}_{\Upsilon(nS)} \equiv \sum_{J=0,1,2}\frac{\sigma(\mathrm{pp}\to\chi_{\mathrm{bJ}}(mP)\mathrm{X})}{\sigma(\mathrm{pp}\to\Upsilon(nS)\mathrm{X})} \times\mathcal{B}[\chi_{\mathrm{bJ}}(mP)\to\Upsilon(nS)], \quad (3)$$

where n and m are radial quantum numbers of the bound states and $\mathcal{B}$ denotes the branching ratios for the decay $\chi_{\mathrm{bJ}}(mP)\to\Upsilon(nS)\gamma$.

To obtain $\mathrm{d}\sigma_{\mathrm{S_zS'_z}}$, similar treatment as in Refs. [10, 17] is taken for both direct and feed-down contributions. For various feed-down contributions in ϒ production, we treat them in different ways to get comparable results. The details are given in the next section.

The newly updated Feynman Diagram Calculation package [22, 23] is used in our calculation. Compared with our former work, the newly added calculations are for the productions of $\chi_{\mathrm{bJ}}(3P)$ under different experimental conditions.

3 Numerical results

In the numerical calculation, the CTEQ6M parton distribution functions [24] and corresponding two-loop QCD coupling constants α_{s} are used. We adopt an approximation $m_{\mathrm{b}}=M_{\mathrm{H}}/2$ for the quark mass, where M_{H} is the mass of bottomonium H. All the masses are taken from the PDG [25], except for $\chi_{\mathrm{bJ}}(3P)$, which is chosen as $M_{\chi_{\mathrm{bJ}}(3P)}$ =10.511 GeV for J=0,1,2 [19]. Therefore, the mass of the bottom quark in our calculation is of different values for $\Upsilon(nS)$ and $\chi_{\mathrm{bJ}}(nP)$.

The color-singlet LDMEs are estimated from wave functions at the origin:

$$\langle\mathcal{O}^{\Upsilon(nS)}(^3S_1^{[1]})\rangle = \frac{9}{2\pi}|R_{\Upsilon(nS)}(0)|^2,$$

$$\langle\mathcal{O}^{\chi_{\mathrm{bJ}}(mP)}(^3P_{\mathrm{J}}^{[1]})\rangle = \frac{3}{4\pi}(2J+1)|R'_{\chi_{\mathrm{b}}(mP)}(0)|^2. \quad (4)$$

The wave functions and their derivatives can be cal-

culated by the potential model [26]. The results are summarized in Table 1.

Branching ratios of $\chi_{bJ}(mP)\to\Upsilon(nS)\gamma$ can be found in Table 1 of Ref. [17]. However, the branching ratio for $\chi_{bJ}(3P)$ is not included there. Since no experimental data for branching ratios of $\chi_{bJ}(3P)$ feed-down to $\Upsilon(nS)$ is available right now, we take $\mathcal{B}[\chi_{bJ}(3P)\to\Upsilon(3S)]\simeq\mathcal{B}[\chi_{bJ}(2P)\to\Upsilon(2S)]$ as an approximation and ignore the contributions from $\chi_{bJ}(3P)$ for $\Upsilon(2S)$ and $\Upsilon(1S)$ due to the small fractions.

Table 1. Radial wave functions at the origin [26].

$\Upsilon(nS)$	$\lvert R_{\Upsilon(nS)}(0)\rvert^2$	$\chi_{bJ}(mP)$	$\lvert R'\chi_{b(mP)}(0)\rvert^2$
$1S$	6.477 GeV^3	$1P$	1.417 GeV^5
$2S$	3.234 GeV^3	$2P$	1.653 GeV^5
$3S$	2.474 GeV^3	$3P$	1.794 GeV^5

The factorization, renormalization and NRQCD scales are chosen as $\mu_f=\mu_r=\sqrt{4m_b^2+p_t^2}$ and $\mu_\Lambda=m_b v\approx$ 1.5 GeV, respectively. The center-of-mass energy is 1.8 TeV and 1.96 TeV for the Tevatron Run I and Run II and, 7 TeV and 8 TeV for the LHC, respectively. A shift $p_t^H\approx p_t^{H'}\times(M_H/M_{H'})$ is used while considering the kinematics effect in the feed-down from higher excited states.

In the fit, we have used three kinds of data from experimental measurements, namely, the differential cross sections from CDF [27], LHCb [28], CMS [29] and ATLAS [30]; the polarization from CDF [31] and CMS [32]; the fractions of $\Upsilon(nS)$ production originating from radiative decays of $\chi_{bJ}(mP)$ meson ($\mathcal{R}^{\chi_b(mP)}_{\Upsilon(nS)}$) [19]. We included the data of the fraction from $\chi_{bJ}(3P)$ feed-down at both $\sqrt{s}$=7 TeV and $\sqrt{s}$=8 TeV in the fit of $\Upsilon(3S)$, while for $\Upsilon(2S)$ and $\Upsilon(1S)$, only the data at $\sqrt{s}$=7 TeV for fractions are included. The linear interpolation method has been taken when dealing with the fraction data since it is thought to behave smoothly and gently for different values of p_t. Only the data in the region $p_t>8$ GeV are used in our fit as we know that the double expansion in α_s and v^2 is not good in the small p_t regions.

Table 2. The obtained CO LDMEs for bottomonia production (in units of 10^{-2} GeV^3). $\chi_{bJ}(3P)$ feed-down contributions are only considered for $\Upsilon(3S)$ with branching ratios $\mathcal{B}[\chi_{bJ}(3P)\to\Upsilon(3S)]\simeq\mathcal{B}[\chi_{bJ}(2P)\to\Upsilon(2S)]$ as an approximation.

state	$\langle\mathcal{O}^{\Upsilon(nS)}(^1S_0^{[8]})\rangle$	$\langle\mathcal{O}^{\Upsilon(nS)}(^3S_1^{[8]})\rangle$	$\langle\mathcal{O}^{\Upsilon(nS)}(^3P_0^{[8]})\rangle/m_b^2$	state	$\langle\mathcal{O}^{\chi_{b0}(mP)}(^3S_1^{[8]})\rangle$
$\Upsilon(1S)$	13.6±2.43	0.61±0.24	−0.93±0.5	$\chi_{b0}(1P)$	0.94±0.06
$\Upsilon(2S)$	0.62±1.98	2.22±0.24	−0.13±0.43	$\chi_{b0}(2P)$	1.09±0.14
$\Upsilon(3S)$	1.45±1.16	1.32±0.20	−0.27±0.25	$\chi_{b0}(3P)$	0.69±0.14

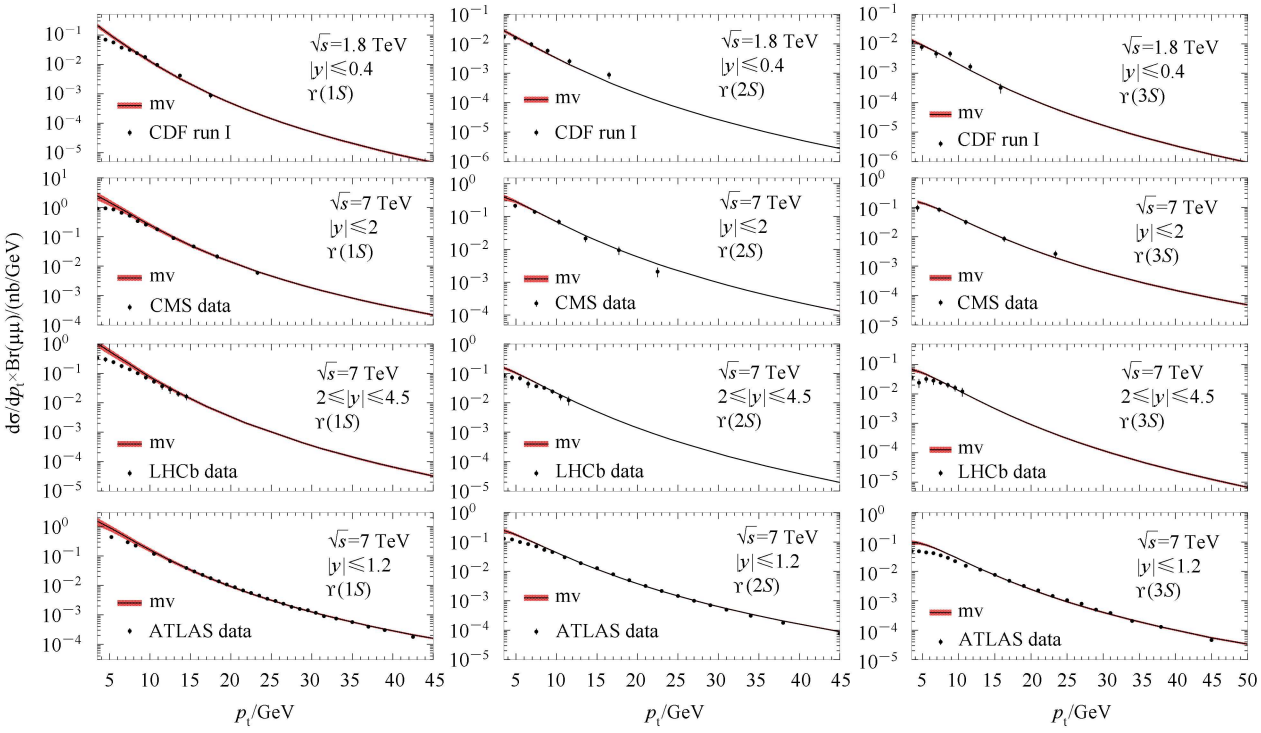

Fig. 1. (color online) Differential cross sections for Υ hadroproduction at the Tevatron and LHC. From left to right: $\Upsilon(1S)$, $\Upsilon(2S)$ and $\Upsilon(3S)$. Rows from top to bottom correspond to different experimental conditions of CDF run I, CMS, LHCb, and ATLAS. The experimental data are collected from Refs. [27–30].

We perform the fits for $\Upsilon(3S)$, $\Upsilon(2S)$, $\Upsilon(1S)$ hadroproduction step-by-step, and the corresponding χ^2/d.o.f are 97/72, 114/47, 73/44. All the fitted CO LDMEs are presented in Table 2. A covariant-matrix method [10] is performed for the plots in order to express the uncertainty from the CO LDMEs properly. We only rotate the three direct LDMEs, however, namely $\langle\mathcal{O}^{\Upsilon(nS)}(^1S_0^8)\rangle$, $\langle\mathcal{O}^{\Upsilon(nS)}(^3S_1^8)\rangle$,$\langle\mathcal{O}^{\Upsilon(nS)}(^3P_J^8)\rangle$, while the last one, $\langle\mathcal{O}^{\chi_{b0}(nP)}(^3S_1^8)\rangle$, is fixed. The descriptions of yield, polarization and fractions are given in the following subsections.

3.1 Yield and polarization

The results for differential cross sections of Υ hadroproduction are shown in Fig. 1, while those for polarization are shown in Fig. 2. The uncertainty bands in the figures are from the errors of the CO LDMEs. The experimental data are stamped with different center-of-mass energy $\sqrt{s}$, rapidity cut and corresponding collaboration in all plots.

We can see from Fig. 1 that the results for the yield of $\Upsilon(nS)$ hadroproduction fit all the experimental measurements very well in a wide p_t range and the uncertainties are very small. In contrast with our previous fit results [17] without $\chi_{bJ}(3P)$ feed-down contributions, where the polarization of $\Upsilon(3S)$ shows a weird steep behaviour and cannot explain the experimental measurement, our updated fits for $\Upsilon(3S)$ have changed a lot, with the contributions of $\chi_{bJ}(3P)$ feed-down for the polarization shown in Fig. 2, and the new results fit the experimental measurements very well. Yet, one may notice that a point at $p_t=7$ GeV in CDF run II deviates from the theory by a long way for $\Upsilon(3S)$ polarization, even worse than in the case without $\chi_{bJ}(3P)$ feed-down in Ref. [17]. This can be understood since the convergence of perturbative expansion is thought to be worse for small p_t range and the data points with $p_t<8$ GeV have been excluded from the fit. For $\Upsilon(2S)$, the production is dominated by the $^3S_1^{[8]}$ channel, which leads to a slightly transverse polarization behaviour ($\lambda\approx0.6$) in the high p_t region. Nevertheless, the results for polarization can explain the CMS data well, but there is still some distance from the CDF experimental data. This is also the case for $\Upsilon(1S)$ polarization, although it is almost unpolarized for the whole p_t region ($0\leqslant\lambda\leqslant0.4$).

3.2 Fractions

In Fig. 3, we give the results for the fractions of $\chi_{bJ}(mP)$ feed-down to $\Upsilon(nS)$. Only four fractions $\mathcal{R}^{\chi_b(3P)}_{\Upsilon(3S)}$, $\mathcal{R}^{\chi_b(2P)}_{\Upsilon(2S)}$, $\mathcal{R}^{\chi_b(1P)}_{\Upsilon(1S)}$, $\mathcal{R}^{\chi_b(2P)}_{\Upsilon(1S)}$ are presented, since in our approximation the $\chi_{bJ}(3P)$ feed-down contributions are ignored for $\Upsilon(1S,2S)$ production. For $\mathcal{R}^{\chi_b(3P)}_{\Upsilon(3S)}$, we give the results at $\sqrt{s}$=7 TeV (black solid line) and $\sqrt{s}$=8 TeV (red dotted line), but they are almost overlapping.

For the other three cases, the results at $\sqrt{s}$=8 TeV are not included since in the experimental measurements they are almost the same as for $\sqrt{s}$=7 TeV [19], and it is believed that theoretical predictions for the fractions are almost unchanged for centre-of-mass energy $\sqrt{s}$=7 TeV and 8 TeV. Our results for $\mathcal{R}^{\chi_b(nP)}_{\Upsilon(nS)}$ show different behaviours for each of n=1,2,3: they are increasing, flat ($p_t>10$ GeV) and slightly decreasing, respectively, as p_t increases. All of them fit the experimental data very

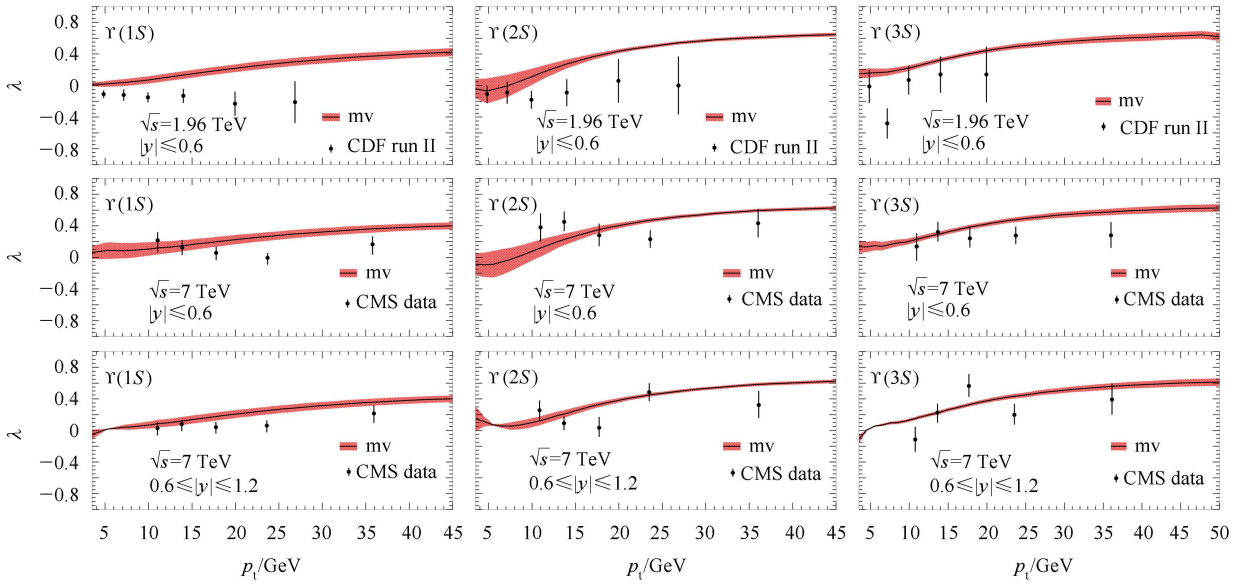

Fig. 2. (color online) Polarization parameter λ for Υ hadroproduction at the Tevatron and LHC. From left to right: $\Upsilon(1S)$, $\Upsilon(2S)$ and $\Upsilon(3S)$. Rows from top to bottom correspond to different experimental conditions of CDF run II, CMS($|y|<0.6$), and CMS($0.6<|y|<1.2$). The experimental data are taken from Refs. [31, 32].

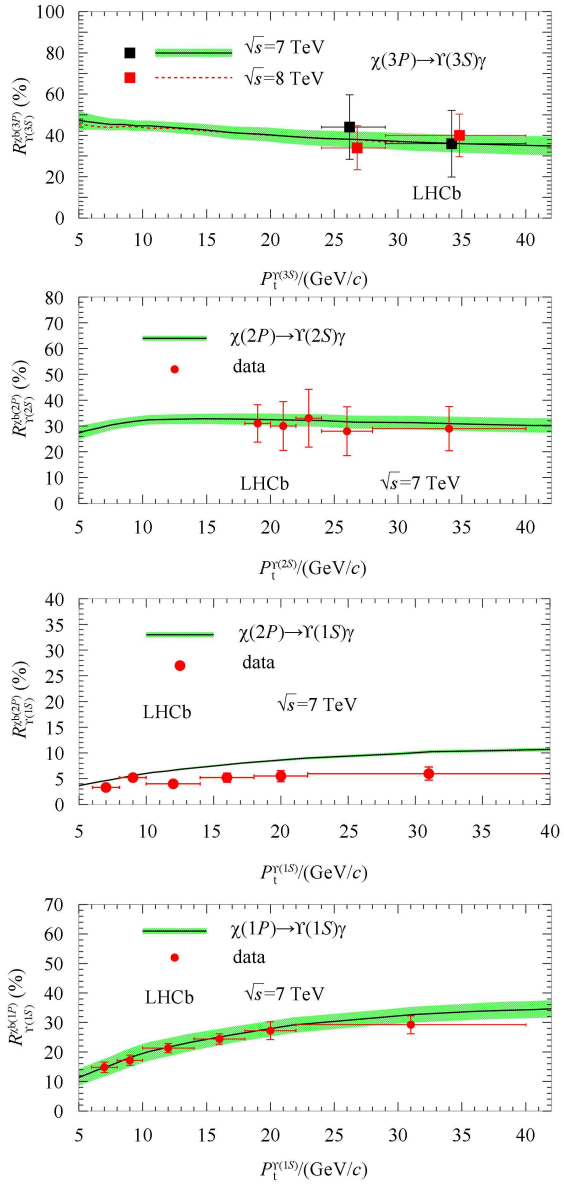

Fig. 3. (color online) Fractions $\mathcal{R}^{\chi_b(mP)}_{\Upsilon(nS)}$ as functions of p_t^{Υ}. From top to bottom: $\mathcal{R}^{\chi_b(3P)}_{\Upsilon(3S)}$, $\mathcal{R}^{\chi_b(2P)}_{\Upsilon(2S)}$, $\mathcal{R}^{\chi_b(2P)}_{\Upsilon(1S)}$, $\mathcal{R}^{\chi_b(1P)}_{\Upsilon(1S)}$. The experimental data are collected from Ref. [19].

well. The remaining fraction $\mathcal{R}^{\chi_b(2P)}_{\Upsilon(1S)}$ shows an increasing behaviour, but the theoretical result overshoots the data by about a factor of two.

3.3 Ratio of $\sigma[\chi_{b2}(1P)]/\sigma[\chi_{b1}(1P)]$

Recently, new measurements of the ratio of cross sections of $\sigma[\chi_{b2}(1P)]$ to $\sigma[\chi_{b1}(1P)]$ were reported by the LHCb [18] and CMS collaborations [20].

As a way of checking our fitting results for the LDMEs, we present the prediction of the cross section ratio $\sigma[\chi_{b2}(1P)]/\sigma[\chi_{b1}(1P)]$ in Fig. 4, where the green band is the results for LHCb experimental conditions while the yellow band is for CMS conditions. As the plot shows, the CMS experimental data can be explained by the theory, while the LHCb data is underestimated. To save the CPU time consumption, the theoretical prediction data with the rapidity range $|y|<1.2$, which is obtained for the fit to yield and polarization, is used to compare with the CMS experimental data [20], where the rapidity range is $|y|<1.5$. We think that it is reasonable to ignore this difference for the ratio result.

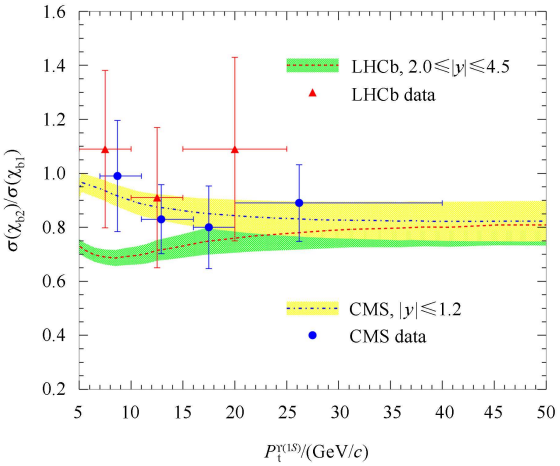

Fig. 4. (color online) The ratio of the cross sections of χ_{b2} to χ_{b1} production, as a function of p_t. The yellow band is the results for CMS while the green one is for LHCb. The experimental data are taken from Refs. [18, 20].

4 More fitting results

While we were preparing this work, a similar work was preprinted by H. Han et al. [33], where they estimated the branching ratios of $\chi_{bJ}(3P)$ feed-down to $\Upsilon(1S,\ 2S,\ 3S)$ and fitted the productions and polarizations. In our fit in the former section, we ignored the $\chi_{bJ}(3P)$ feed-down contributions for $\Upsilon(1S,\ 2S)$ since they are very small. Giving a more rigorous treatment of the feed-down contributions would be instructive. Meanwhile, the NRQCD factorization scale μ_Λ dependence does exist at the fixed order results. To explore the uncertainties from these two aspects, we refit the production and polarization and obtain two sets of new LDMEs for $\mu_\Lambda = m_b v = 1.5$ GeV and $\mu_\Lambda = m_b$ together with the branching ratios $\mathcal{B}[\chi_{bJ}(3P) \to \Upsilon(nS)]$ estimated in Ref. [33] Table I, and the numerical results are presented in Table 3 and Table 4 respectively.

For convenience, we define three short statements,

1) default scheme ($\mu_\Lambda = m_b v = 1.5$ GeV and our naive estimation for branching ratios $\mathcal{B}[\chi_{bJ}(3P) \to \Upsilon(3S)] = \mathcal{B}[\chi_{bJ}(2P) \to \Upsilon(2S)]$, $\mathcal{B}[\chi_{bJ}(3P) \to \Upsilon(1S,\ 2S)] = 0$),

2) Han's scheme ($\mu_\Lambda = m_b$ and branching ratios $\mathcal{B}[\chi_{bJ}(3P) \to \Upsilon(nS)]$ estimated in Ref. [33] Table 1),

3) mixed scheme ($\mu_\Lambda = m_b v = 1.5$ GeV and branching ratios $\mathcal{B}[\chi_{bJ}(3P) \to \Upsilon(nS)]$ estimated in Ref. [33] Table 1).

For the mixed scheme in Table 3, some changes compared with the default scheme in Table 2 should be mentioned. For $\Upsilon(3S)$, the dominant CO channel becomes $^3S_1^{[8]}$ and the numerical value for $\langle \mathcal{O}^{\chi_{b0}(3P)}(^3S_1^{[8]})\rangle$ becomes larger. This is not at all a surprise since we know the branching ratios $\mathcal{B}[\chi_{bJ}(3P) \to \Upsilon(3S)]$ used in the default scheme are much larger than they are in the mixed scheme. This difference is consistent with the different decay branching ratios being used. For $\Upsilon(2S)$ and $\Upsilon(1S)$, the LDMEs values have smaller changes.

In comparison with the mixed scheme, for Han's scheme in Table 4, the LDMEs for $\Upsilon(2S)$ change a lot because the $^1S_0^{[8]}$ channel becomes negative and the $^3P_J^{[8]}$ channel gives positive contributions. In addition, the value of $\langle \mathcal{O}^{\chi_{b0}(1P)}(^3S_1^{[8]})\rangle$ becomes larger, which may impact the behaviour of the ratio $\sigma[\chi_{b2}(1P)]/\sigma[\chi_{b1}(1P)]$.

The results of the yield and polarization in both Han's scheme and the mixed scheme are almost the same as those in the default scheme. In all three schemes, the

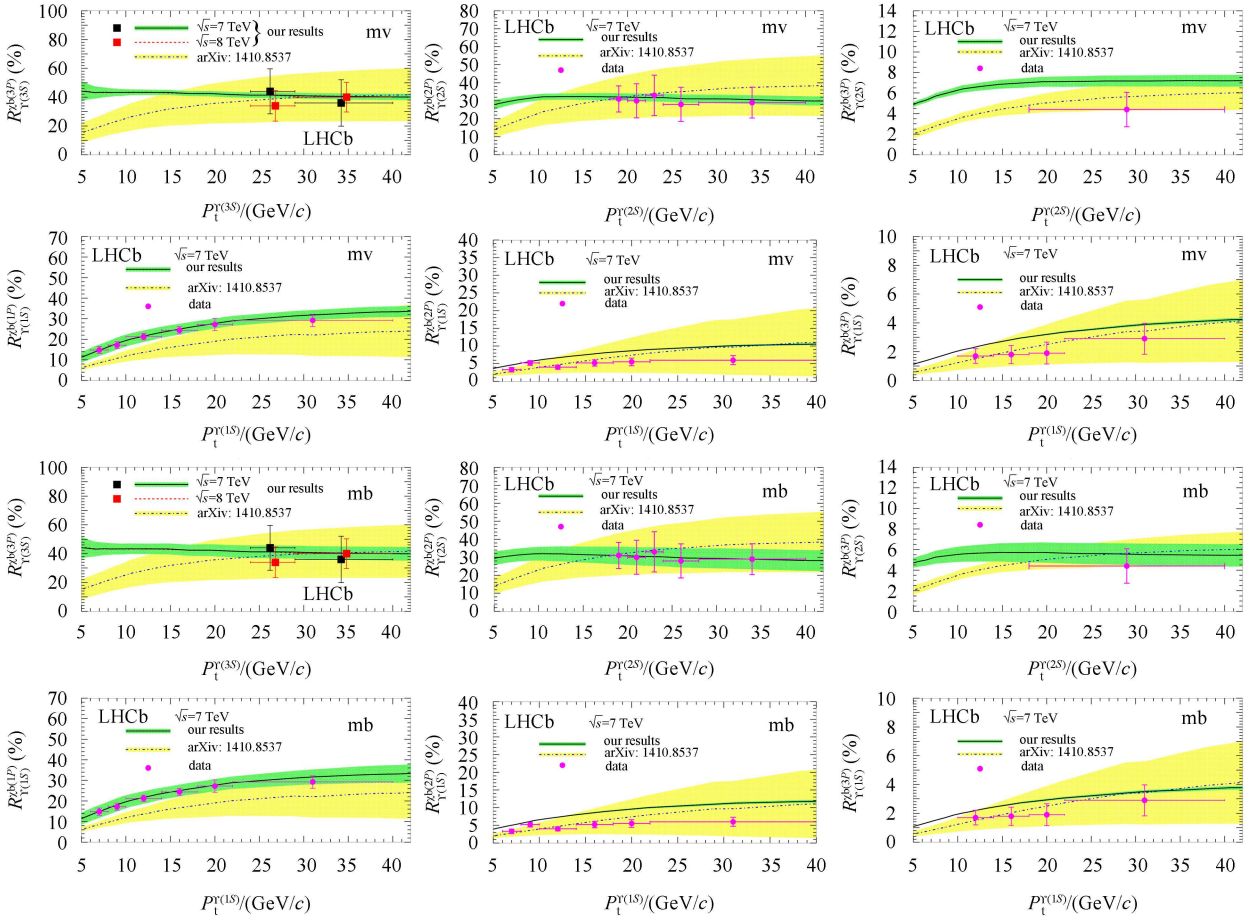

Fig. 5. (color online) Fractions $\mathcal{R}^{\chi_b(mP)}_{\Upsilon(nS)}$ as functions of p_t^Υ. The green bands are our predictions, with the upper two rows being the results for the Table 3 mixed scheme and the lower two rows are for Table 4, Han's scheme. The yellow bands are obtained by using the LDMEs in Ref. [33]. From left to right: $\mathcal{R}^{\chi_b(3P)}_{\Upsilon(3S)}$, $\mathcal{R}^{\chi_b(2P)}_{\Upsilon(2S)}$, $\mathcal{R}^{\chi_b(3P)}_{\Upsilon(2S)}$ in the first and third row and $\mathcal{R}^{\chi_b(1P)}_{\Upsilon(1S)}$, $\mathcal{R}^{\chi_b(2P)}_{\Upsilon(1S)}$, $\mathcal{R}^{\chi_b(3P)}_{\Upsilon(1S)}$ in the second and fourth row. The experimental data are collected from Ref. [19].

Table 3. Same as Table 2, except that we choose the branching ratio $\mathcal{B}[\chi_{bJ}(3P) \to \Upsilon(nS)]$ in Ref. [33], so-called mixed scheme.

state	$\langle \mathcal{O}^{\Upsilon(nS)}(^1S_0^{[8]})\rangle$	$\langle \mathcal{O}^{\Upsilon(nS)}(^3S_1^{[8]})\rangle$	$\langle \mathcal{O}^{\Upsilon(nS)}(^3P_0^{[8]})\rangle/m_b^2$	state	$\langle \mathcal{O}^{\chi_{b0}(mP)}(^3S_1^{[8]})\rangle$
$\Upsilon(1S)$	10.1±2.23	0.73±0.22	−0.23±0.50	$\chi_{b0}(1P)$	0.91±0.06
$\Upsilon(2S)$	1.19±1.93	1.88±0.23	−0.01±0.42	$\chi_{b0}(2P)$	1.07±0.12
$\Upsilon(3S)$	−0.15±0.90	1.53±0.12	−0.02±0.19	$\chi_{b0}(3P)$	1.76±0.14

Table 4. Same as Table 3, except that we choose $\mu_\Lambda = m_b$, Han's scheme.

state	$\langle\mathcal{O}^{\Upsilon(nS)}(^1S_0^{[8]})\rangle$	$\langle\mathcal{O}^{\Upsilon(nS)}(^3S_1^{[8]})\rangle$	$\langle\mathcal{O}^{\Upsilon(nS)}(^3P_0^{[8]})\rangle/m_b^2$	state	$\langle\mathcal{O}^{\chi_{b0}(mP)}(^3S_1^{[8]})\rangle$
$\Upsilon(1S)$	11.6±2.61	0.47±0.41	−0.49±0.59	$\chi_{b0}(1P)$	1.16±0.07
$\Upsilon(2S)$	−0.59±2.31	2.94±0.40	0.28±0.52	$\chi_{b0}(2P)$	1.50±0.21
$\Upsilon(3S)$	−0.18±1.40	1.52±0.33	−0.01±0.30	$\chi_{b0}(3P)$	1.92±0.34

yield results describe the experimental data very well for the polarization of CMS measurement, but not the CDF measurements. We do not show these plots here to avoid unnecessary repetition, since there is little difference compared with the results in the default scheme shown in Fig. 1 (for yield) and Fig. 2 (for polarization).

In Fig. 5, we present all the results for the fractions of $\chi_{bJ}(mP)$ feed-down to $\Upsilon(nS)$ obtained by using the LDMEs in the mixed scheme and Han's scheme. The green bands are our fitted results while the yellow bands are obtained by using the LDMEs in Ref. [33].

We summarize the results in two parts. First, the results show little difference for the fractions between Han's scheme and the mixed scheme, except for $\mathcal{R}^{\chi_b(3P)}_{\Upsilon(2S)}$, for which in Han's scheme the band is closer to the data. Since the only difference between the two fitting schemes is the choice of NRQCD factorization scale μ_Λ, it indicates the scale dependence for μ_Λ is small for the fixed order correction. Second, we show the difference between our results and Han's results in Ref. [33]. In their results, the $\chi_{bJ}(mP)$ feed-down contributions tend to increase as p_t goes higher for all $\Upsilon(nS)$. In our results, however, only the fractions $\mathcal{R}^{\chi_b(1P,2P,3P)}_{\Upsilon(1S)}$ keep increasing behaviour for all three schemes, and the other fractions show a slight decrease or smooth behaviour. Meanwhile, with a large uncertainty band, Han's results can cover all the experimental data except for $\chi_{bJ}(1P)$ to $\Upsilon(1S)$, where their results underestimated the data slightly. Our results present a somewhat interesting case, with the results in our three schemes giving a good explanation for the fractions $\mathcal{R}^{\chi_b(mP)}_{\Upsilon(nS)}$ for $m=n=1,2,3$, while overestimating the data by a factor of less than two for the other fractions where $m\neq n$.

We present the ratio of cross sections $\sigma[\chi_{b2}(1P)]/\sigma[\chi_{b1}(1P)]$ for Han's scheme in Fig. 6, while the results for the mixed scheme are not presented to avoid repetition, since they are indistinguishable with those for the default scheme shown in Fig. 4 due to the almost identical value of $\langle\mathcal{O}^{\chi_{b0}(1P)}(^3S_1^{[8]})\rangle$ (see Table 2 and Table 3).

It can be seen that the value of $\langle\mathcal{O}^{\chi_{b0}(1P)}(^3S_1^{[8]})\rangle$ in Table 4 for Han's scheme is larger than that in Table 2 for the default scheme. With this value, the $\chi_{b2}(1P)$ and $\chi_{b1}(1P)$ ratio predictions in Fig. 6 for Han's scheme describe the experimental measurements better than those in Fig. 4 for the default scheme, and the results cover all the CMS data very well, while only one point for the LHCb measurements is inside the error band. Nevertheless, this difference can be explained as the uncertainty of the NRQCD factorization scale. In our results for both CMS and LHCb, all the centre values of the ratio $\sigma[\chi_{b2}(1P)]/\sigma[\chi_{b1}(1P)]$ are less than 1, or equally, there is a relation $\sigma[\chi_{b2}(1P)]<\sigma[\chi_{b1}(1P)]$. This is the case for the CMS experimental data. But for LHCb, the value at two points out of the three are bigger than 1. From this point of view, the prediction might be inconsistent with LHCb data. However, we cannot come to that conclusion for the ratio here due to the limited LHCb data.

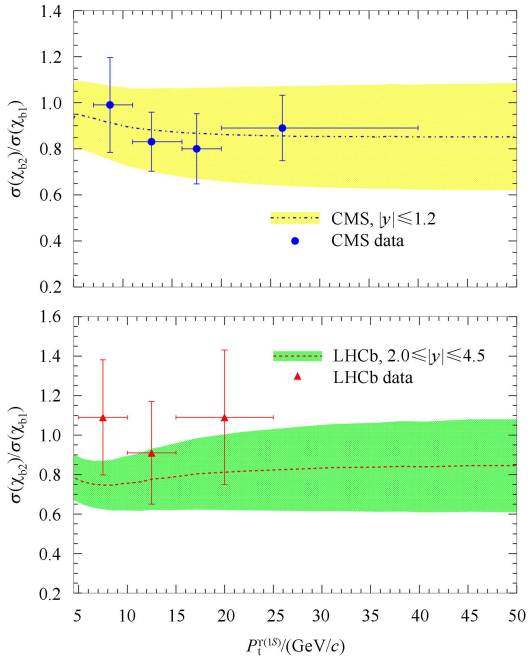

Fig. 6. (color online) The same as Fig. 4, except that the LDME $\langle\mathcal{O}^{\chi_{b0}(1P)}(^3S_1^{[8]})\rangle$ in Table 4 is used.

5 Summary

In this work, we presented an updated study on the yield and polarization of $\Upsilon(1S, 2S, 3S)$. In contrast to our previous study [17] without $\chi_{bJ}(3P)$ feed-down contributions, there are two new points: $\chi_{bJ}(3P)$ feed-down contributions are taken into consideration by using available measurements of $\chi_{bJ}(3P)$; the experimental measurements of the fraction of $\chi_{bJ}(2P,1P)$ feed-down are available and applied in our fit. We obtain the CO LDMEs for Υ hadroproduction by fitting the experimental data for yield, polarization and fractions at the

Tevaron and LHC step-by-step. To further explore the uncertainty from the NRQCD factorization scale μ_Λ dependence and different choice of the $\chi_{bJ}(3P)$ feed-down ratios, we have performed fits in three schemes by using different NRQCD factorization scale μ_Λ and $\chi_{bJ}(3P)$ feed-down ratios.

All the obtained results can explain the transverse momentum distribution of production rate very well, just as in in our previous work. For polarization, the results of $\Upsilon(3S)$ at large p_t can reproduce the experimental data, which proves the emphasis in our previous work that the the $\chi_{bJ}(3P)$ feed-down could be very important for $\Upsilon(3S)$ polarization. The behavior for $\Upsilon(1S,2S)$ changes little with the addition of $\chi_{bJ}(3P)$ feed-down. The polarizations results can explain the CMS data well, but the distance from CDF data cannot be ignored. The results for the fraction $\mathcal{R}^{\chi_b(nP)}_{\Upsilon(nS)}$ show different behaviours for each of $n = 1,2,3$: they are increasing, flat (p_t>10 GeV) and slightly decreasing respectively as p_t increases, and all of them fit the experimental data well. We also presented our prediction for the ratio $\sigma[\chi_{b2}(1P)]/\sigma[\chi_{b1}(1P)]$, which can reproduce the CMS measurements well, but slightly underestimates the LHCb data.

In our study of the uncertainty with three schemes, we find that different choices of $\chi_{bJ}(3P)$ feed-down ratios hardly modify the final results, since its effect is almost renormalized by its CO LDME $\langle\mathcal{O}^{\chi_{b0}(3P)}(^3S_1^{[8]})\rangle$, which is dominant over its color-singlet part (the value is fixed). Therefore this study cannot distinguish which choice of $\chi_{bJ}(3P)$ feed-down ratios is better, and only with further experimental measurements of $\chi_{bJ}(3P)$ hadroproduction can the feed-down ratio be fixed.

Furthermore, we find that the uncertainty from the NRQCD factorization scale μ_Λ dependence is noticeable in our fit and predication. The important fact is that there are sizeable differences for the obtained CO LDMEs in the fits between different choices of NRQCD factorization scale, although the fitted results are almost the same. The different CO LDMEs sets can bring large differences in predictions at other experiments such as ee, ep colliders. The uncertainty is because the matching between NRQCD and QCD cannot be made exactly in the fixed-order perturbative calculation, which has also been observed and discussed in previous work [34, 35]. It must therefore be taken into consideration in result presentations or global fits.

We thank Dr. H-F. Zhang for helpful discussions.

References

1 Braaten E, Fleming S. Phys. Rev. Lett., 1995, **74**: 3327–3330
2 Bodwin G T, Braaten E, Lepage G P. Phys. Rev. D, 1995, **51**: 1125–1171
3 Campbell J M, Maltoni F, Tramontano F. Phys. Rev. Lett., 2007, **98**: 252002
4 GONG Bin, WANG Jian-Xiong. Phys. Rev. Lett., 2008, **100**: 232001
5 KANG Zhong-Bo, QIU Jian-Wei, Sterman G. Phys. Rev. Lett., 2012, **108**: 102002
6 GONG Bin, LI Xue-Qian, WANG Jian-Xiong. Phys. Lett. B, 2009, **673**: 197–200
7 MA Yan-Qing, WANG Kai, CHAO Kuang-Ta. Phys. Rev. D, 2011, **83**: 111503
8 Butenschoen M, Kniehl B A. Phys. Rev. Lett., 2012, **108**: 172002
9 CHAO Kuang-Ta, MA Yan-Qing, SHAO Hua-Sheng et al. Phys. Rev. Lett., 2012, **108**: 242004
10 GONG Bin, WAN Lu-Ping, WANG Jian-Xiong et al. Phys. Rev. Lett., 2013, **110**: 042002
11 Aaij R et al. (LHCb collaboration). arXiv: 1409.3612
12 Butenschoen M, HE Zhi-Guo, Kniehl B A. Phys. Rev. Lett., 2014, **114**: 092004
13 HAN Hao, MA Yan-Qing, MENG Ce et al. Phys. Rev. Lett., 2015, **114**: 092005
14 ZHANG Hong-Fei, SUN Zhan, SANG Wen-Long et al. Phys. Rev. Lett., 2014, **114**: 092006
15 GONG Bin, WANG Jian-Xiong, ZHANG Hong-Fei. Phys. Rev. D, 2011, **83**: 114021
16 WANG Kai, MA Yan-Qing, CHAO Kuang-Ta. Phys. Rev. D, 2012, **85**: 114003
17 GONG Bin, WAN Lu-Ping, WANG Jian-Xiong et al. Phys. Rev. Lett., 2014, **112**(3): 032001
18 Aaij R et al. (LHCb collaboration). JHEP, 2014, **1410**: 88
19 Aaij R et al. (LHCb collaboration). Eur. Phys. J. C, 2014, **74**(10): 3092
20 Khachatryan V et al. (CMS collaboration). arXiv: 1409. 5761
21 Beneke M, Kramer M, Vanttinen M. Phys. Rev. D, 1998, **57**: 4258–4274
22 WANG Jian-Xiong. Nucl. Instrum. Methods A, 2004, **534**: 241–245
23 WAN Lu-Ping, WANG Jian-Xiong. Comput. Phys. Commun, 2014, **185**: 2939–2949
24 Pumplin J, Stump D R, Huston J et al. JHEP, 2002, **0207**: 012
25 Beringer J et al. (Particle Data Group collaboration). Phys. Rev. D, 2012, **86**: 010001
26 Eichten E J, Quigg C. Phys. Rev. D, 1995, **52**: 1726–1728
27 Acosta D et al. (CDF collaboration). Phys. Rev. Lett., 2002, **88**: 161802
28 Aaij R et al. (LHCb collaboration). Eur. Phys. J. C, 2012, **72**: 2025
29 Khachatryan V et al. (CMS collaboration). Phys. Rev. D, 2011, **83**: 112004
30 Aad G et al. (ATLAS collaboration). Phys. Rev. D, 2013, **87**(5): 052004
31 Aaltonen T et al. (CDF collaboration). Phys. Rev. Lett., 2012, **108**: 151802
32 Chatrchyan S et al. (CMS collaboration). Phys. Rev. Lett., 2013, **110**(8): 081802
33 HAN Hao, MA Yan-Qing, MENG Ce et al. arXiv:1410.8537
34 WANG Jian-Xiong, ZHANG Hong-Fei. J. Phys. G, 2015, **42**(2): 025004
35 JIA Lan, YU Ling, ZHANG Hong-Fei. arXiv: 1410.4032